Preprints.org

Article

Not peer-reviewed version

CEA-Functionalized Gold Nanoparticles as a Nanovaccine Platform: In Vitro Evaluation of Cytocompatibility, Cellular Uptake, and Antigen Processing

Razvan Septimiu Zdrehus , Teodora Mocan * , Lavinia Ioana Sabau , Cristian Tudor Matea , Flaviu Tăbăran , Teodora Pop , Cristian Delcea * , Ofelia Mosteanu , Lucian Mocan

Posted Date: 12 May 2025

doi: 10.20944/preprints202505.0830.v1

Keywords: gold nanoparticles (AuNPs); carcinoembryonic antigen (CEA); nanovaccine; cancer immunotherapy

Preprints.org is a free multidisciplinary platform providing preprint service that is dedicated to making early versions of research outputs permanently available and citable. Preprints posted at Preprints.org appear in Web of Science, Crossref, Google Scholar, Scilit, Europe PMC.

Copyright: This open access article is published under a Creative Commons CC BY 4.0 license, which permit the free download, distribution, and reuse, provided that the author and preprint are cited in any reuse.

Preprints.org (www.preprints.org) | NOT PEER-REVIEWED | Posted: 12 May 2025 doi:10.20944/preprints202505.0830.v1

Disclaimer/Publisher's Note: The statements, opinions, and data contained in all publications are solely those of the individual author(s) and contributor(s) and not of MDPI and/or the editor(s). MDPI and/or the editor(s) disclaim responsibility for any injury to people or property resulting from any ideas, methods, instructions, or products referred to in the content.

Article

CEA-Functionalized Gold Nanoparticles as a Nanovaccine Platform: In Vitro Evaluation of Cytocompatibility, Cellular Uptake, and Antigen Processing

Razvan Zdrehus[2],, Teodora Mocan*[3,2], Lavinia Ioana Sabau,[3], Cristian Tudor Matea[2,4], Flaviu Tabaran[5], Teodora Pop[1,6], Cristian Delcea*[1,6], Ofelia Mosteanu[1,6] and Lucian Mocan[1,2]

[1] 3rd Surgery Clinic, "Iuliu Hatieganu" University of Medicine and Pharmacy, Cluj Napoca, Romania
[2] Nanomedicine Department, Regional Institute of Gastroenterology and Hepatology, "Iuliu Hatieganu" University of Medicine and Pharmacy Cluj Napoca, Romania
[3] Physiology Department, "Iuliu Hatieganu" University of Medicine and Pharmacy, Cluj Napoca, Romania
[4] Department of Biosciences, University of Salzburg, Hellbrunnerstraße 34, 5020, Salzburg, Austria
[5] Department of Pathology, Sciences and Veterinary Medicine, University of Agricultural, ClujNapoca, Romania
[6] Department of Gastroenterology "Iuliu Hatieganu" University of Medicine and Pharmacy, ClujNapoca, Romania
* Correspondence to: Teodora Mocan, e-mail: teodora.mocan@umfcluj.ro, Cristian Delcea email: cristian.delcea.cj@gmail.com Tel.: +40 264 439696 Fax +40 264 439696

Abstract: **Background and aim.** The efficacy of cancer vaccines depends on the development of safe and effective delivery systems that can improve antigen stability, facilitate targeted uptake by immune cells, and promote efficient intracellular processing. Gold nanoparticles offer an attractive platform due to their biocompatibility, stability, and modifiable surfaces. Functionalizing gold nanoparticles with tumor-associated antigens such as carcinoembryonic antigen (CEA) peptides may enhance antigen presentation and stimulate immune activation. This study aimed to evaluate the cytocompatibility, cellular internalization, and antigen-processing capabilities of CEA-functionalized gold nanoparticles (CEA-AuNPs) as a potential nanovaccine candidate in vitro. **Materials and Methods.** CEA peptides were conjugated to gold nanoparticles and characterized using UV-VIS spectroscopy and dynamic light scattering to confirm functionalization and assess particle size distribution. In vitro assays were performed on macrophage cell cultures to evaluate cytotoxicity (via viability and caspase-3 expression), nanoparticle uptake (by reflectance microscopy), and antigen processing (via fluorescence intensity analysis). **Results.** Spectral analysis confirmed successful functionalization, with a broadened absorbance plateau between 510–700 nm and a size increase from 20 nm (bare AuNPs) to ~80 nm (CEA-AuNPs). Viability assays demonstrated cytologyc viability above 85% at all tested concentrations. Caspase-3 activity, suggested controlled apoptotic signaling in response to the nanoconstruct. Reflective imaging and fluorescence microscopy confirmed efficient cellular uptake, localized predominantly in the perinuclear region, and enhanced proteasomal activity in macrophages treated with the CCEA-AuNPs, indicating effective antigen processing. **Discussion.** Functionalization of gold nanoparticles with a CEA peptide resulted in stable, biocompatible nanostructures capable of efficient uptake by antigen-presenting cells. Enhanced intracellular processing, evidenced by increased ubiquitin-proteasome pathway activity, highlights the immunogenic potential of the construct. Low cytotoxicity supports its suitability for further preclinical development. **Conclusion** CEA-functionalized gold nanoparticles exhibit high cytocompatibility, targeted cellular uptake, and promote intracellular antigen processing—highlighting their promise as a nanovaccine platform in cancer immunotherapy. These results support further preclinical evaluation toward translational application.

© 2025 by the author(s). Distributed under a Creative Commons CC BY license.

Preprints.org (www.preprints.org) | NOT PEER-REVIEWED | Posted: 12 May 2025 doi:10.20944/preprints202505.0830.v1

Keywords: gold nanoparticles (AuNPs); carcinoembryonic antigen (CEA); nanovaccine; cancer immunotherapy

1. Introduction

Cancer remains one of the leading causes of morbidity and mortality globally, accounting for millions of deaths each year despite advances in conventional therapies such as surgery, chemotherapy, and radiotherapy [1]. The limitations of these traditional approaches—including systemic toxicity, drug resistance, and lack of tumor specificity—underscore the urgent need for innovative treatment strategies that can selectively target tumor cells, while minimizing harm to normal tissues [2]. Among emerging alternatives, cancer immunotherapy, particularly therapeutic vaccination, has gained increasing attention for its potential to harness the body's immune system to recognize, target, and eliminate malignant cells [3, 4].

Cancer vaccines aim to prime the immune system against tumor-specific or tumor-associated antigens (TAAs), promoting a robust and lasting antitumor response [5]. Carcinoembryonic antigen (CEA), a well-studied TAA, is a glycoprotein normally produced at very low levels in healthy adults but overexpressed in a wide range of epithelial tumors. These include colorectal, gastric, pancreatic, lung, and breast cancers, among others [6]. CEA plays a role in cell adhesion and is involved in cancer progression and metastasis, making it a valuable biomarker and therapeutic target in oncology [7]. Its elevated expression in various adenocarcinomas underlies its use in cancer diagnosis, prognosis, and monitoring treatment response [8]. Its restricted expression in normal adult tissues and its immunogenic potential make CEA a favorable candidate for vaccine development [9].

A major challenge in designing effective cancer vaccines is the efficient delivery of antigens to immune cells in a way that preserves antigen structure, enhances cellular uptake, and stimulates a strong immune response [5]. Traditional vaccine formulations often suffer from poor antigen uptake, rapid clearance, and suboptimal delivery to lymph nodes, leading to weak and short-lived immunity [4].

Nanotechnology offers transformative solutions to these delivery challenges [10]. Among nanomaterials, gold nanoparticles (AuNPs) are particularly attractive as vaccine carriers due to their high surface-area-to-volume ratio, excellent biocompatibility, ease of synthesis and functionalization, and the ability to tailor their size and surface properties [11]. These unique physicochemical features enable AuNPs to efficiently carry and present antigens, protect them from degradation, and promote their uptake by antigen-presenting cells, enhancing the magnitude and duration of the antitumor immune response [12].

AuNPs can be functionalized with a wide variety of biological molecules, including peptides, proteins, and nucleic acids, allowing for the development of multifunctional nanoconstructs that not only carry tumor antigens but also incorporate targeting ligands or immunostimulatory agents [13]. Furthermore, their optical properties make them useful for real-time tracking of cellular interactions and biodistribution [14]. When used in a vaccine context, AuNPs can facilitate multivalent antigen presentation, potentially enhancing receptor engagement on antigen-presenting cells (APCs) and promoting effective activation of both innate and adaptive immunity [15].

In this study, we report the synthesis and functionalization of AuNPs with a peptide derived from CEA to serve as a proof-of-concept nanovaccine candidate. We performed a comprehensive physicochemical characterization of the resulting nano-bio-construct and evaluated its cellular uptake, cytotoxicity, and antigen-processing potential in vitro using macrophage cell culturess. Through spectroscopic, microscopic, and biological assays, we demonstrate the favorable characteristics of the CEA-AuNP construct and its capacity to engage immune cells. This work sets the stage for future in vivo investigations aimed at developing effective and targeted nanoparticle-based cancer vaccines.

© 2025 by the author(s). Distributed under a Creative Commons CC BY license.

Preprints.org (www.preprints.org) | NOT PEER-REVIEWED | Posted: 12 May 2025 doi:10.20944/preprints202505.0830.v1

2. Materials and Methods

2.1. Synthesis and characterization of gold nanoparticles

We used the Turkevich method to obtain gold nanoparticles (AuNPs) with specific properties [16]. In the first step, 40 mg of gold tetrachloride trihydrate ($HAuCl_4$-$3H_2O$) trihydrate ($HAuCl_4$-$3H_2O$) was dissolved in bidistilled water. The resulting solution was brought to boiling, thus providing the necessary thermal conditions for the reaction. Subsequently, 5 mL of a solution of sodium citrate (20 mg/mL) was added with continuous stirring. The reaction was maintained for 2 hours to allow complete formation of nanoparticles, after which the mixture was allowed to cool to room temperature.

The synthesized nanoparticles were characterized by a number of analytical techniques, including UV-Vis spectroscopy, FT-IR spectroscopy, dynamic light scattering (DLS) and atomic force microscopy (AFM).

UV-Vis spectroscopy was performed with a Shimadzu UV-1800™ spectrophotometer in the range 200-800 nm with a spectral resolution of 0.5 nm. Spectra for AuNP, AuNP-TA and AuNP-TA-IgG samples were normalized using OriginLab® 7.0 software.

The hydrodynamic size and size distribution of the nanoparticles were determined by DLS using a Zetasizer Nano S90 instrument (Malvern Instruments, Westborough, UK) operated at an angle of 90° and at a temperature of 20°C.

Fourier transform infrared (FT-IR) spectroscopy was performed with a Perkin-Elmer Spectrum Two® spectrometer equipped with attenuated total reflectance (ATR) mode, and the obtained data were analyzed with Spectrum 10™ software.

Morphological characterization of nanoparticles was performed by AFM using a TT-AFM® system (AFMWorkshop, CA, USA) operated in non-contact mode with ACTA-SS (AppNano, CA, USA) tips. Samples were deposited on mica substrates using a KLM® SCC spin-coater, and the obtained images were processed with Gwyddion® 2.36 software.

2.2. Functionalization of gold nanoparticles with colon cancer targeting molecule.

We started from the nanostructure solution described above. In order to expose available functional groups binding to AuNPs, a first step was performed to reduce the peptides used (CEA; source -MyBiosource.com). Thus, an amount of 150 µL of peptide was diluted with 1mL distilled H2O. 100mM DTT (dithiothreitol) reagent was used. After adding the reducing reagent, the reaction was allowed to continue for 1 hour at room temperature. In the next step, 1 mL AuNP solution and 9 mL ultrapure water were added. The pH was adjusted to 7. Under continuous stirring, the reaction continued for 2 hours at room temperature. At the end of the reaction, purification steps were carried out by ultracentrifugation (over 10000 rpm) for 15 minutes and redispersion in distilled water.

UV-VIS spectral characterization was performed using a Shimadzu UV-1800® spectrophotometer. Recording parameters were between 300-700mm and normalization was performed using the OriginLab® 7.0 software package.

The Zetasizer-Nano S90 (Malvern Instruments, Westborough, UK) was used to determine the hydrodynamic particle diameter (DLS) using a diffraction angle of 90 degrees and a temperature of 25^0C .

The determination of the spectral fingerprint of the synthesized nanocomposite was carried out using a TT-AFM® system (AFMWorkshop, CA, USA). After recording, the data were processed using the Gwyddion® 2.36 software package.

2.3. In vitro studies - cell suspension preparation and maintenance

RAW 264.7 cells, obtained by purchase, were in a first step subjected to the thawing step, subsequently the culture was maintained by specific procedures.

© 2025 by the author(s). Distributed under a Creative Commons CC BY license.

Preprints.org (www.preprints.org) | NOT PEER-REVIEWED | Posted: 12 May 2025 doi:10.20944/preprints202505.0830.v1

2.3.1. Thawing procedure:

The following steps were followed according to the standards indicated by the producer. A step of equilibration of the growth medium (RAWGM1) was carried out by transferring it into a T75 flask and maintaining it for 30 minutes at controlled temperature and atmosphere (37°C, 5% CO2). Manipulations of the culture and growth medium were carried out according to aseptic rules. The rapid temperature increase step was performed by immersing the cryogenic vial in a marine bath at 37°C until complete thawing. The cell pellet was resuspended in 9mL of medium using a 15mL conical tube, followed by cell reseparation by centrifugation at 3500rpm for 5 minutes at room temperature, followed by removal of supernatant except for a minimal amount (5-10 µl). The medium was then supplemented by adding 10mL of new culture medium with cell resuspension by repetitive pipetting through multiple aspirate-discharge sequences. The cell suspension was transferred to a 25mL flask with placement in an incubator with parameters of 37°C temperature and 5% CO2.

At an interval of 48 h steps of medium replacement with 5 -10mL fresh, pre-equilibrated (30 min) and pre-warmed (37°C) fresh medium were performed. The technique involved careful aspiration after tilting the culture flask of the medium with the addition of new, pre-conditioned medium. It was verified that the new medium level covered the cells

Also, after removal of the used medium, the steps necessary to resuspend the cells in the new medium were performed. For this, EDTA solution (0.48 mM) was added in a volume of 5mL and the culture flask was placed in the incubator for 2 minutes. At the end of the interval, contact of the cells with the pre-warmed EDTA solution (37°C) was ensured, especially at the periphery of the culture by rotating the flask at 90 degrees, in a repetitive manner. The step was continued with repetitive pipetting (aspiration-discharge), using a 10mL pipette of the solution, in order to completely dislodge the cells from the bottom of the culture flask. Repetitive rinsing of the culture dish was performed in order to remove cells and generate a complete cell suspension. Care was taken to prevent the introduction of air bubbles by pipetting and suspension handling. The cell suspension was collected in a new 15 mL conical tube.

The culture was placed in a stable culture vessel after cell separation by centrifugation (3500rpm, 5min, room temperature). The EDTA solution was aspirated. Cell counting steps were performed using Tripan Blue dye. It was then blotted in separate flasks at a calculated density of 1X105/flask. Uniformization of the cell density was achieved by successive pipetting-discharge sessions. The culture vessels were placed in a humidified atmosphere at 37°C and 5%CO2 content.

2.3.2. Maintenance procedure:

At 7-10 days interval, the culture required separation by sub-culture. Prior to any use of the culture medium, the medium pre-conditioning steps (37°C, 5% CO2, 30 min) were performed. Culture flasks were removed from the incubator. A mechanical cell removal device was used to remove cells from the bottom of the flask. Cells and medium were collected by gently tilting the flask and aspirating into a 10mL disposable pipette. Cell capital transfer was carried out with extreme caution to avoid introducing additional air bubbles. The contents were transferred into a 15mL conical tube.

Separation of the cell component from the medium was performed by centrifugation (3500rpm, 25°C, 5 minutes). The culture medium used was removed with the addition of new, pre-conditioned medium. The new culture suspension was homogenized by ascending-descending pipetting, and the inoculation was performed after previous calculation of cell density.

At intervals of 3-4 days steps of medium addition were performed, with the removal of 1/3 of the volume of used culture medium and replacement with fresh, pre-conditioned medium.

2.4. In vitro exposure of the cell suspension to the vaccine nanoconstruct

The exposure of macrophage culture to the functionalizatized product AuNP- CEA was serially performed. Comparative acute exposure experiments of the cell culture to PBS and different

© 2025 by the author(s). Distributed under a Creative Commons CC BY license.

Preprints.org (www.preprints.org) | NOT PEER-REVIEWED | Posted: 12 May 2025 doi:10.20944/preprints202505.0830.v1

concentrations of nanomaterial (50µg/mL, 25µg/mL, 12.5µg/ mL) were performed. The evaluation of cell internalization was performed using Cytoviva equipment, dark-field microscopy technique with white light reflectance, by visualizing the reflection spots originating from the nanoparticulate component (AuNP) of the newly generated structure.

The MTT assay [17], based on the formation of a colorimetrically detectable compound by viable cells, was used to assess cell viability/proliferation. The analysis was performed in triplicate, after exposures performed on the culture inoculated in 96-well plates. The apoptosis level was quantified by the level of caspase 3 in the cell lysate.

2.5. Evaluation of antigen trafficking in the exposed cell suspension

To investigate the ability of macrophages to process the antigenic complex carried by gold nanoparticles, macrophage culture was exposed to the nanostructured compound. Subsequently, the behavior of the nanostructure in its interaction with macrophage cells was analyzed.

Antigen processing was evaluated using the Proteostat® labeling kit (Enzo Life Sciences), specific for the detection of proteins degraded by the ubiquitin-proteasome pathway. The analysis was performed by fluorescence microscopy using an FSX100 microscope equipped with a rhodamine filter, which allowed accurate visualization of protein aggregates resulting from antigen processing.

3. Results

3.1. Synthesis and characterization of gold nanoparticles

The UV-VIS spectral fingerprint of the resulting colloidal solution revealed a distinct absorbance maximum centered at 522 nm (Figure 1, a), which is characteristic of the surface plasmon resonance (SPR) of spherical gold nanoparticles (AuNPs) in the 20 nm size range. This sharp and symmetrical peak indicates the successful synthesis of well-dispersed, unaggregated nanoparticles with uniform morphology. The absence of additional peaks or peak broadening suggests minimal aggregation and high colloidal stability of the AuNP suspension.

Complementary to the spectroscopic findings, hydrodynamic size analysis performed using dynamic light scattering (DLS) confirmed the presence of a monodisperse population of nanoparticles, with an average diameter of approximately 20 nm (Figure 1, b). The low polydispersity index (PDI) obtained from this measurement further supports the uniformity of the particle population, corroborating the UV-VIS data and indicating precise control over the synthesis process. This size range is particularly favorable for biomedical applications, including cellular uptake and antigen delivery, due to its optimal interaction with biological membranes and immune cells.

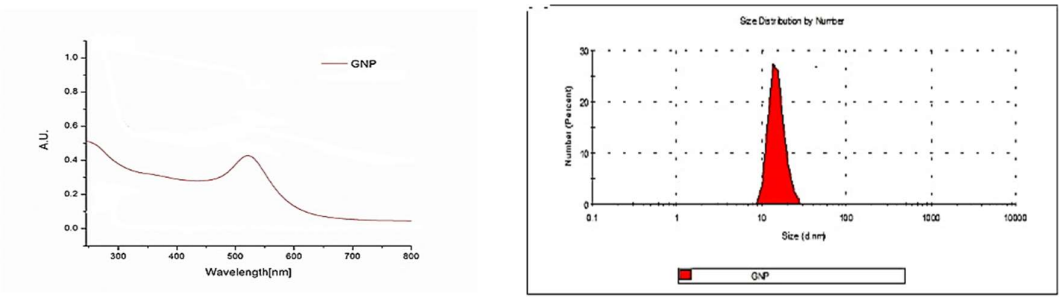

(**a**) (**b**)

Figure 1. UV-VIS spectral fingerprint of AuNPs (a). Spectroscopy: hydrodynamic size analysis (b)

© 2025 by the author(s). Distributed under a Creative Commons CC BY license.

Preprints.org (www.preprints.org) | NOT PEER-REVIEWED | Posted: 12 May 2025 doi:10.20944/preprints202505.0830.v1

3.2. Functionalization. Physical and chemical characterization of the CEA-AuNP.

The UV-VIS spectral fingerprint of the solution containing the functionalized product exhibited a notable alteration in absorbance characteristics compared to the unmodified gold nanoparticles. Specifically, instead of a sharp and narrow absorbance peak centered at 522 nm—typical for spherical, monodisperse gold nanoparticles—the spectrum showed a broad and inhomogeneous shoulder extending from approximately 510 to 700 nm (Figure 2.a). This broadened spectral profile, often described as a plateau or shoulder, is indicative of changes in the local refractive index surrounding the nanoparticles and is consistent with successful surface functionalization. The altered spectral shape results from the superimposition of the intrinsic plasmonic peak of the gold nanoparticle core and additional absorbance contributions from the attached biomolecular ligands, in this case, the CEA-derived peptide. Such changes are commonly observed when proteins or peptides are conjugated to metallic nanoparticles, affecting their dielectric environment and light-scattering behavior.

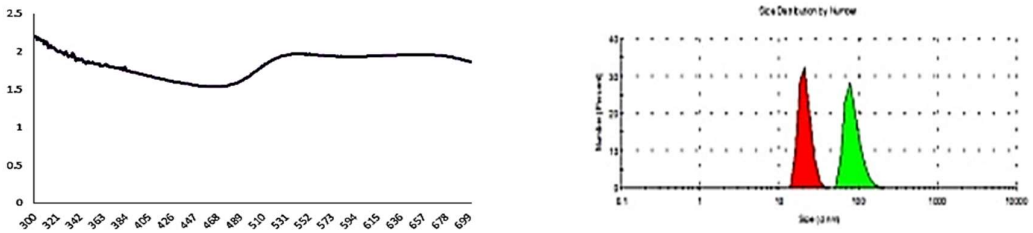

(**a**) (**b**)

Figure 2. Evaluation of AuNP functional molecule binding. UV-Vis spectre after functionalization (a). Hydrodynamic dimension (d.nm) : red- AuNP , Green- CEA-AuNP (b).

In parallel, hydrodynamic size analysis revealed a distinct shift in nanoparticle diameter following functionalization (Figure 2.b). The average size increased from the initial 20 nm (observed for unmodified AuNPs) to approximately 80 nm for the CEA-functionalized nanoparticles, while still maintaining a monodisperse distribution. This size augmentation is indicative of the successful conjugation of the peptide moiety to the nanoparticle surface, contributing additional hydrodynamic volume. The overlaid DLS profiles further illustrate this shift, with the original nanoparticle population represented in red and the functionalized construct shown in green. The broader size distribution observed post-functionalization suggests some variability in the number of peptides bound per nanoparticle, which is typical in biofunctionalization protocols. Nevertheless, the retention of monodispersity confirms that aggregation did not occur, and the overall formulation remains stable—a critical factor for biomedical applicability.

3.3. In vitro exposure of the cell suspension to the vaccine nanoconstruct

The results presented in Figure 3 demonstrate that cell viability and proliferation levels remained consistently high, even at the maximum tested concentration of the functionalized nanostructure. Specifically, the viability values exceeded 85%, a threshold generally considered acceptable for biomedical applications, including those intended for human use. This indicates that the CEA-AuNPs exhibit a favorable cytocompatibility profile under the conditions tested, and do not elicit significant cytotoxic effects at relevant experimental doses.

© 2025 by the author(s). Distributed under a Creative Commons CC BY license.

Preprints.org (www.preprints.org) | NOT PEER-REVIEWED | Posted: 12 May 2025 doi:10.20944/preprints202505.0830.v1

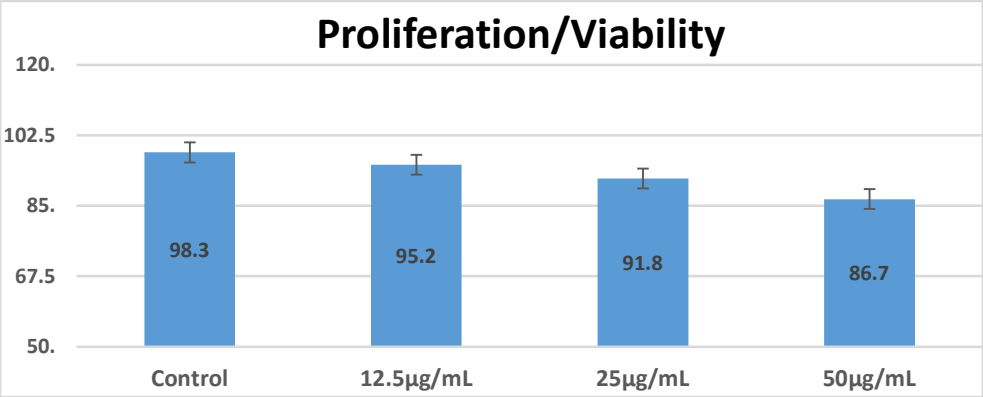

Figure 3. A slight decrease in viability is observed in proportion to the increase in exposure concentration.

This reduction was modest and did not fall below critical viability levels, suggesting that the decrease is likely attributable to dose-dependent cellular stress rather than overt toxicity.

Apoptosis levels, assessed by caspase-3 quantification in cell lysates, indicated activation of apoptotic mechanisms (Figure 4). The observed activation suggests the engagement of intrinsic apoptotic signaling cascades, which often involve mitochondrial membrane permeabilization and the subsequent release of cytochrome C. These events culminate in the activation of initiator caspases (such as caspase-9), which in turn activate effector caspases like caspase-3.

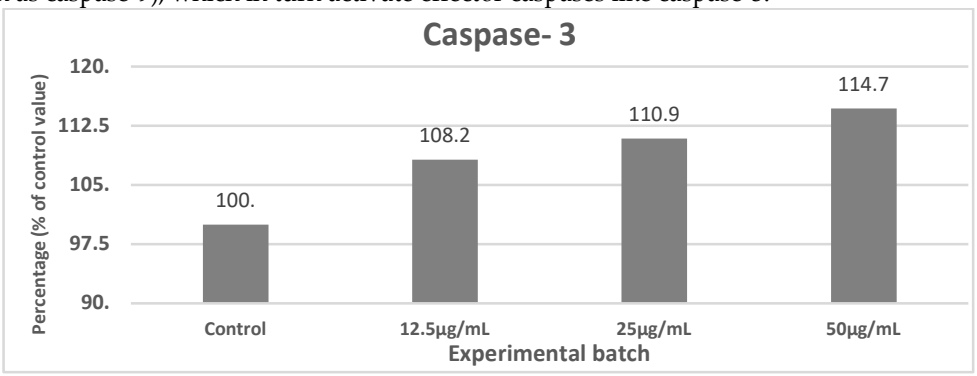

Figure 4. A direct proportionality is observed between the nanomaterial concentration and the level of caspase-3.

Notably, this activation pattern was predominantly observed in the test groups treated with the CEA-AuNPs, suggesting that the nanoconjugate may selectively influence apoptotic pathways, possibly through antigen recognition or intracellular stress signaling mechanisms. These findings align with the broader safety and efficacy profile of the nanovaccine candidate, indicating controlled apoptotic response rather than widespread cellular toxicity.

The overall trend supports the biocompatibility of the CEA-AuNP formulation and provides encouraging evidence for its potential safe use in therapeutic contexts, such as cancer vaccination strategies, where repeated or systemic administration may be required.

These findings are crucial in the preclinical assessment of nanomaterials, as high levels of cell viability in vitro are a prerequisite for proceeding toward in vivo studies and, eventually, clinical translation.

3.4. Assessment of antigen processing by macrophages

Exposure of the macrophage culture to the nanostructured compound, followed by subsequent analysis of this interaction, revealed clear evidence of nanoparticle internalization. This was

© 2025 by the author(s). Distributed under a Creative Commons CC BY license.

Preprints.org (www.preprints.org) | NOT PEER-REVIEWED | Posted: 12 May 2025 doi:10.20944/preprints202505.0830.v1

visualized by the presence of distinct reflection spots within the cells, originating from the metallic AuNP component of the newly synthesized nanostructure (Figure 5). These spots, discernible through reflective light microscopy, serve as optical signatures of the nanoparticulate presence and provide strong evidence of cellular uptake.

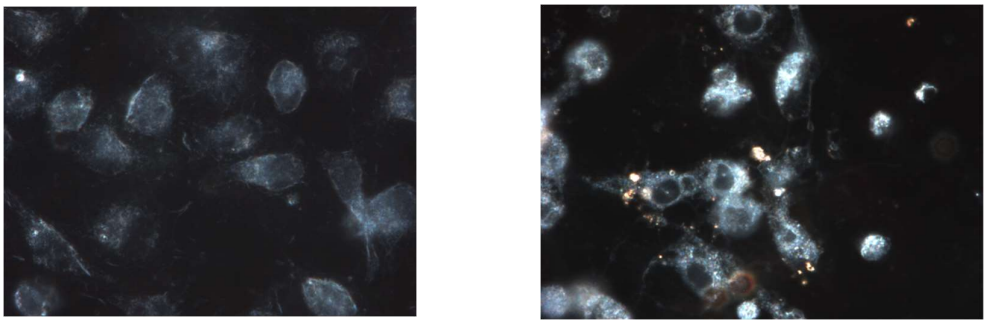

Control 50µg/mL CEA-AuNP

Figure 5. Dark field microscopy with white light reflectance. (Cytoviva).

The presence of numerous and concentrated reflection spots within the cytoplasmic compartment—especially around the perinuclear region—implies a spatially organized internalization pattern. The observed localization, characterized by a dense accumulation near but not within the nucleus, supports the hypothesis that the nanostructures are being trafficked toward endosomal or proteasomal compartments, which are typically positioned in the perinuclear zone. Interestingly, the nuclear area itself remains devoid of such reflectance, reinforcing the idea of targeted subcellular localization.

The levels and intensity of fluorescent signal emission in the red spectrum were carefully evaluated following exposure of the macrophage cells to the nanostructured compound. The cultures treated with CEA-AuNP, 50 µg/mL, exhibited a markedly increased presence of distinct red fluorescent emission spots, as opposed to control groups exposed to unfunctionalized AuNPs (Figure 6).

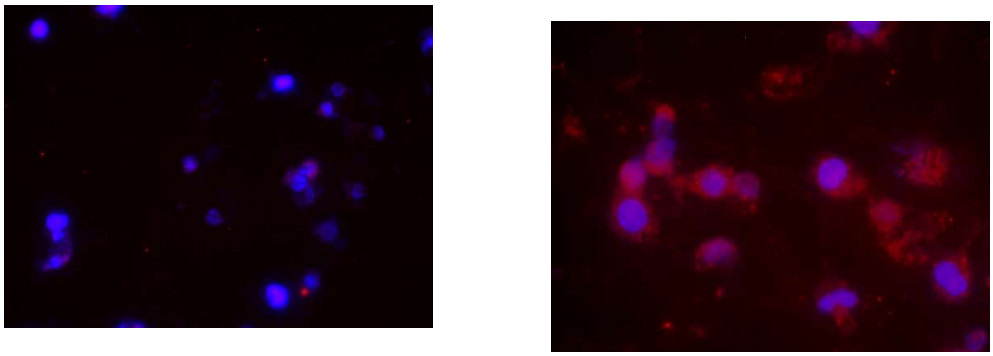

Control lot 50µg/mL CEA-AuNP

Figure 6. Fluorescence microscopy (FSX100 microscope with rhodamine filter).

This elevated fluorescent signal is indicative of enhanced proteasomal activity and indicate intracellular antigen processing. The finding suggests that the nanostructured compound facilitates a more efficient delivery and subsequent intracellular routing of the antigen toward degradation and presentation pathways, particularly via the ubiquitin-proteasome system.

© 2025 by the author(s). Distributed under a Creative Commons CC BY license.

Preprints.org (www.preprints.org) | NOT PEER-REVIEWED | Posted: 12 May 2025 doi:10.20944/preprints202505.0830.v1

4. Discussion

The development of effective cancer vaccines hinges not only on the identification of suitable tumor-associated antigens but also on the optimization of delivery systems capable of enhancing antigen stability, presentation, and uptake by immune cells [5, 10, 18]. In this context, our findings provide valuable insights into the structural and functional characteristics of a nanovaccine construct based on AuNPs functionalized with a CEA peptide [9]. The results presented in this study offer compelling evidence for the biocompatibility, internalization, and immunological activation potential of CEA-AuNP system, proposed as a nanovaccine platform for tumor antigen delivery.

The results obtained from the synthesis and characterization of the nanostructures highlight the success of the Turkevich method in generating a stable nanostructured product with controlled dimensions and potential for further functionalization[19]. The presence of the absorption maximum around 522 nm in the UV-Vis spectrum, together with the monodispersed distribution around 20 nm, confirms the obtaining of small, homogeneous gold nanoparticles, as is specific for this classical colloidal synthesis method [20].

Spectroscopic analysis using UV-VIS revealed significant modifications in the absorbance profile following functionalization with CEA. While unmodified AuNPs exhibited the expected narrow surface plasmon resonance (SPR) peak centered at 522 nm, the functionalized construct demonstrated a broadened absorbance plateau ranging from 510 to 700 nm. This shift is consistent with changes in the local refractive index surrounding the nanoparticles, caused by the peptide corona [21]. Such spectral transformations are frequently associated with successful bioconjugation, as the protein or peptide layers alter the dielectric environment and introduce new absorbance contributions [22]. These findings support the hypothesis that CEA was successfully immobilized on the nanoparticle surface, creating a stable bio-nanoconjugate with modified optical properties [23].

Hydrodynamic diameter measurements further confirmed the efficiency of the functionalization process [24]. The observed increase in average particle size from ~20 nm (unmodiffied AuNPs) to ~80 nm for the CEA-AuNP complex suggests the presence of a surface-bound organic layer, consistent with the addition of the antigenic peptide. The size range of ~80 nm is within the optimal window for uptake by antigen-presenting cells, such as macrophages and dendritic cells, which are instrumental in the initiation of adaptive immune responses [25, 26].

Notably, despite the increase in particle size, the system retained a monodisperse distribution, indicating that aggregation was effectively prevented—a critical factor for biological stability, biodistribution, and immunological safety [27]. A mild broadening of the size distribution was noted, which is typical in protein or peptide surface conjugation, where variability in molecular loading across the nanoparticle population occurs [28, 29].

The in vitro studies assesing CEA-AuNP cytotoxicity in the macrophage cell culture revealed high levels of cell viability and proliferation across all tested concentrations of the nanoconstruct, with values exceeding 85%—a benchmark widely recognized as acceptable for biomedical applications [30-32]. This favorable cytocompatibility profile, even at the upper experimental concentration limit (50 μg/mL), underscores the structural safety of the CEA-AuNP formulation. The slight, dose-dependent decrease in viability observed did not fall below critical thresholds and is likely indicative of mild cellular stress rather than overt toxicity [33, 34]. These results are encouraging for further translational development, particularly for vaccine strategies requiring systemic or repeated administration, where long-term tolerance and minimal adverse effects are important [35].

The analysis of apoptosis through caspase-3 activation further supports the notion of controlled cellular responses [36]. Caspase-3 is a key executioner protease in the apoptotic pathway, and its elevated expression or activation is a hallmark of programmed cell death [37]. We observe a direct proportionality between the nanomaterial concentration and the caspase-3 level. The activation of caspase-3 observed in our study, with a predominantly perinuclear localization, is consistent with

© 2025 by the author(s). Distributed under a Creative Commons CC BY license.

Preprints.org (www.preprints.org) | NOT PEER-REVIEWED | Posted: 12 May 2025 doi:10.20944/preprints202505.0830.v1

early events in intrinsic apoptosis. Previous research has shown that mitochondrial clustering around the nucleus facilitates the release of pro-apoptotic factors such as cytochrome c, leading to efficient activation of caspase-3 [38, 39]. This pattern supports the hypothesis that the nanoconstruct initiates apoptosis through mitochondrial-mediated pathways, a mechanism critical for controlled cell death without inducing inflammatory responses [40, 41]. The spatial distribution aligns with earlier findings from apoptosis assays, where activation of caspase-3 was also noted predominantly in the perinuclear region, hinting at a functional correlation between antigen processing and apoptotic signaling pathways [42]. Such targeted activation is advantageous in immunotherapeutic contexts, where mild apoptosis may assist in the maturation and antigen-presenting functions of dendritic cells and macrophages, ultimately enhancing T-cell priming [43].

Macrophage internalization studies revealed the uptake of the CEA-AuNPs, as evidenced by distinct reflection signals derived from the gold nanoparticle core. These reflectance-based signatures confirmed the intracellular presence and trafficking of the nanoconstruct, with a characteristic accumulation in the perinuclear area. This subcellular distribution aligns with the typical localization of proteasomal and endosomal compartments, which are responsible for the degradation and processing of antigenic peptides [44, 45]. The nuclear region remained devoid of nanoparticulate signals, thus reinforcing the conclusion that the compound avoids genotoxic interaction and instead follows a deffined intracellular processing route [46].

Fluorescence imaging, performed using rhodamine-filtered microscopy, revealed markedly elevated signal intensity in the macrophage cultures treated with the CEA-AuNPs compared to controls. This enhancement correlates with heightened proteasomal activity, which is essential for the processing of endogenous antigens and their subsequent loading onto major histocompatibility complex (MHC) class I molecules [47, 48]. The red fluorescence signal, concentrated in the cytoplasm and especially enriched near the perinuclear zone, suggests active engagement of the ubiquitin-proteasome pathway, a key element in effective antigen presentation and adaptive immune activation [49, 50]. The intensity and widespread distribution of the red fluorescent signals suggest that the processed peptide fragments are likely being loaded onto MHC class I molecules within the endoplasmic reticulum for subsequent presentation on the cell surface. These findings collectively support the dual role of the CEA-AuNP system: as an efficient intracellular delivery vehicle and as a potent stimulator of antigen processing pathways.

The intracellular and intracytoplasmic localization of the nanostructured compound—confirmed through both reflective imaging and fluorescence emission—supports its suitability for vaccine applications. The ability of the metallic gold core to serve as both a delivery scaffold and a detectable marker enhances the traceability of the compound during cellular interactions. This ensures that the antigenic payload is not only internalized but also apropriately directed for effective antigen presentation by macrophages, a critical step in the initiation of adaptive immune responses. This aspect is critical for future in vivo applications where biodistribution, retention, and immunogenicity must be quantitatively assessed.

In the broader context of cancer immunotherapy, these results validate the potential of nanoparticle-based antigen delivery systems to overcome several limitations associated with conventional vaccine platforms, such as poor cellular uptake, antigen degradation, and suboptimal immune activation. By demonstrating safety, intracellular targeting, and efficient antigen processing in vitro, the CEA-AuNP formulation advances toward in vivo preclinical evaluation with a strong foundational profile.

Further investigations should include assessments of dendritic cell activation, antigen-specific T-cell responses, and tumor regression in animal models. The conclusions of the data analyzed so far support the opportunity to continue the experiments in the macrophage- adenocarcinoma cell co-culture platform. Additionally, long-term biocompatibility and immunogenic memory will need to be addressed to fully elucidate the translational potential of this nanovaccine candidate.

The study is limited by the lack of in vivo testing. Future steps include testing in animal models to assess therapeutic efficacy and safety profile.

© 2025 by the author(s). Distributed under a Creative Commons CC BY license.

Preprints.org (www.preprints.org) | NOT PEER-REVIEWED | Posted: 12 May 2025 doi:10.20944/preprints202505.0830.v1

5. Conclusions

The functionalized gold nanoparticles developed in this study demonstrate structural stability, favorable size for cellular uptake, and successful conjugation with the target peptide antigen. These physicochemical characteristics are of particular relevance to translational applications [51].

These findings represent an essential preclinical step in evaluating the therapeutic viability of nanostructured immunotherapies targeting cancer-associated antigens. In this case, the CEA-AuNP structure has the ability to function as an efficient platform for antigen delivery and processing in antigen-presenting cells while maintaining a favorable biocompatibility profile.

Future work will focus on assessing the immunostimulatory effects of this nanovaccine in relevant in vivo models and exploring its potential synergy with adjuvants or checkpoint inhibitors in the context of combinatorial cancer immunotherapy [52, 53].

Author Contributions: All authors have contributed equally to this work. Their involvement includes the conception and design of the study, data acquisition, analysis, and interpretation, as well as drafting the manuscript and critically revising it for important intellectual content. All authors have reviewed and approved the final version for publication. Each author accepts full responsibility for every aspect of the work, ensuring the accuracy and integrity of the entire study. Should any questions arise regarding the reliability or validity of any component, all authors are committed to promptly investigating and resolving such issues.

Funding: This research received no external funding

Acknowledgments: The authors used artificial intelligence (AI)-based tools, including ChatGPT (OpenAI), DeepL Translator, and Perplexity AI, to assist with language editing, phrasing suggestions, and improving manuscript clarity. No AI tool was used for data analysis, scientific interpretation, or decision-making. All intellectual content, analysis, and conclusions are the original work of the authors, who assume full responsibility for the integrity and accuracy of the manuscript.

Conflicts of Interest: The authors declare no conflicts of interest.

Abbreviations

The following abbreviations are used in this manuscript:

AuNP	Gold nanoparticle
CEA	Carcinoembrionic Antigen
CEA-AuNP	CEA functionalized gold nanoparticles
MHC	Major histocompatibility complex

References

1. Bray F, Laversanne M, Sung H, Ferlay J, Siegel RL, Soerjomataram I, et al. Global cancer statistics 2022: GLOBOCAN estimates of incidence and mortality worldwide for 36 cancers in 185 countries. CA: A Cancer Journal for Clinicians. 2024;74(3):229–63.
2. Wang X, Zhang H, Chen X. Drug resistance and combating drug resistance in cancer. Cancer Drug Resist. 2019;2(2):141–60.
3. Fan T, Zhang M, Yang J, Zhu Z, Cao W, Dong C. Therapeutic cancer vaccines: advancements, challenges and prospects. Signal Transduction and Targeted Therapy. 2023;8(1):450.
4. Kaczmarek M, Poznańska J, Fechner F, Michalska N, Paszkowska S, Napierała A, et al. Cancer Vaccine Therapeutics: Limitations and Effectiveness-A Literature Review. Cells. 2023;12(17).
5. Sobhani N, Scaggiante B, Morris R, Chai D, Catalano M, Tardiel-Cyril DR, et al. Therapeutic cancer vaccines: From biological mechanisms and engineering to ongoing clinical trials. Cancer Treat Rev. 2022;109:102429.

© 2025 by the author(s). Distributed under a Creative Commons CC BY license.

Preprints.org (www.preprints.org) | NOT PEER-REVIEWED | Posted: 12 May 2025 doi:10.20944/preprints202505.0830.v1

6. Kankanala VL ZM, Mukkamalla SKR. Carcinoembryonic Antigen. [Updated 2024 Dec 11]. In: StatPearls [Internet]. Treasure Island (FL): StatPearls Publishing; 2025 Jan-. Available from: https://www.ncbi.nlm.nih.gov/books/NBK578172/.
7. Hall C, Clarke L, Pal A, Buchwald P, Eglinton T, Wakeman C, et al. A Review of the Role of Carcinoembryonic Antigen in Clinical Practice. Ann Coloproctol. 2019;35(6):294–305.
8. Choi SH, Yang SY, Han YD, Cho MS, Hur H, Lee KY, et al. Carcinoembryonic antigen levels of tumor-draining venous blood as a prognostic marker in colon cancer. Korean J Clin Oncol. 2017;13(2):68–74.
9. Bhagat A, Lyerly HK, Morse MA, Hartman ZC. CEA vaccines. Hum Vaccin Immunother. 2023;19(3):2291857.
10. Wen R, Umeano AC, Kou Y, Xu J, Farooqi AA. Nanoparticle systems for cancer vaccine. Nanomedicine (Lond). 2019;14(5):627–48.
11. Almeida JP, Figueroa ER, Drezek RA. Gold nanoparticle mediated cancer immunotherapy. Nanomedicine. 2014;10(3):503–14.
12. Almeida JPM, Lin AY, Figueroa ER, Foster AE, Drezek RA. In vivo gold nanoparticle delivery of peptide vaccine induces anti-tumor immune response in prophylactic and therapeutic tumor models. Small. 2015;11(12):1453–9.
13. Cao-Milan R, Liz-Marzan LM. Gold nanoparticle conjugates: recent advances toward clinical applications. Expert Opin Drug Deliv. 2014;11(5):741–52.
14. Liu M, Li Q, Liang L, Li J, Wang K, Li J, et al. Real-time visualization of clustering and intracellular transport of gold nanoparticles by correlative imaging. Nature Communications. 2017;8(1):15646.
15. Mocan T, Matea C, Tabaran F, Iancu C, Orasan R, Mocan L. In Vitro Administration of Gold Nanoparticles Functionalized with MUC-1 Protein Fragment Generates Anticancer Vaccine Response via Macrophage Activation and Polarization Mechanism. J Cancer. 2015;6(6):583–92.
16. Kimling J, Maier M, Okenve B, Kotaidis V, Ballot H, Plech A. Turkevich method for gold nanoparticle synthesis revisited. J Phys Chem B. 2006;110(32):15700–7.
17. Ghasemi M, Turnbull T, Sebastian S, Kempson I. The MTT Assay: Utility, Limitations, Pitfalls, and Interpretation in Bulk and Single-Cell Analysis. Int J Mol Sci. 2021;22(23).
18. Zdrehus R, Delcea C, Mocan L. Role of Biofunctionalized Nanoparticles in Digestive Cancer Vaccine Development. Pharmaceutics. 2024;16(3).
19. Turkevich J, Stevenson PC, Hillier J. A study of the nucleation and growth processes in the synthesis of colloidal gold. Discussions of the Faraday Society. 1951;11(0):55–75.
20. Daniel M-C, Astruc D. Gold Nanoparticles: Assembly, Supramolecular Chemistry, Quantum-Size-Related Properties, and Applications toward Biology, Catalysis, and Nanotechnology. Chemical Reviews. 2004;104(1):293–346.
21. Humbert C, Pluchery O, Lacaze E, Tadjeddine A, Busson B. Optical spectroscopy of functionalized gold nanoparticles assemblies as a function of the surface coverage. Gold Bulletin. 2013;46:299–309.
22. Thambiraj S, Hema S, Shankaran DR. Functionalized gold nanoparticles for drug delivery applications. Materials Today: Proceedings. 2018;5(8):16763–73.
23. Huang X, Jain PK, El-Sayed IH, El-Sayed MA. Gold nanoparticles: interesting optical properties and recent applications in cancer diagnostics and therapy. Nanomedicine. 2007;2(5):681–93.
24. Saenmuangchin R, Siripinyanond A. Flow field-flow fractionation for hydrodynamic diameter estimation of gold nanoparticles with various types of surface coatings. Analytical and bioanalytical chemistry. 2018;410(26):6845–59.
25. Kang S, Ahn S, Lee J, Kim JY, Choi M, Gujrati V, et al. Effects of gold nanoparticle-based vaccine size on lymph node delivery and cytotoxic T-lymphocyte responses. J Control Release. 2017;256:56–67.
26. Nguyen B, Tolia NH. Protein-based antigen presentation platforms for nanoparticle vaccines. npj Vaccines. 2021;6(1):70.
27. Wei Y, Quan L, Zhou C, Zhan Q. Factors relating to the biodistribution & clearance of nanoparticles & their effects on in vivo application. Nanomedicine. 2018;13(12):1495–512.
28. Modena MM, Rühle B, Burg TP, Wuttke S. Nanoparticle characterization: what to measure? Advanced Materials. 2019;31(32):1901556.

© 2025 by the author(s). Distributed under a Creative Commons CC BY license.

Preprints.org (www.preprints.org) | NOT PEER-REVIEWED | Posted: 12 May 2025 doi:10.20944/preprints202505.0830.v1

29. Narayan R, Gadag S, Garg S, Nayak UY. Understanding the effect of functionalization on loading capacity and release of drug from mesoporous silica nanoparticles: a computationally driven study. ACS omega. 2022;7(10):8229–45.
30. Baharara J, Ramezani T, Divsalar A, Mousavi M, Seyedarabi A. Induction of apoptosis by green synthesized gold nanoparticles through activation of caspase-3 and 9 in human cervical cancer cells. Avicenna journal of medical biotechnology. 2016;8(2):75.
31. McNamara K, Tofail SA. Nanoparticles in biomedical applications. Advances in Physics: X. 2017;2(1):54–88.
32. Bharathala S, Sharma P. Biomedical applications of nanoparticles. Nanotechnology in modern animal biotechnology: Elsevier; 2019. p. 113–32.
33. Johnson S, Nguyen V, Coder D. Assessment of cell viability. Current protocols in cytometry. 2013;64(1):9.2. 1–9.2. 26.
34. Conners CM, Bhethanabotla VR, Gupta VK. Concentration-dependent effects of alendronate and pamidronate functionalized gold nanoparticles on osteoclast and osteoblast viability. Journal of Biomedical Materials Research Part B: Applied Biomaterials. 2017;105(1):21–9.
35. Grippin AJ, Sayour EJ, Mitchell DA. Translational nanoparticle engineering for cancer vaccines. Oncoimmunology. 2017;6(10):e1290036.
36. Ma W, Jing L, Valladares A, Mehta SL, Wang Z, Li PA, et al. Silver nanoparticle exposure induced mitochondrial stress, caspase-3 activation and cell death: amelioration by sodium selenite. International journal of biological sciences. 2015;11(8):860.
37. Asadi M, Taghizadeh S, Kaviani E, Vakili O, Taheri-Anganeh M, Tahamtan M, et al. Caspase-3: structure, function, and biotechnological aspects. Biotechnology and Applied Biochemistry. 2022;69(4):1633–45.
38. Frank S, Gaume B, Bergmann-Leitner ES, Leitner WW, Robert EG, Catez F, et al. The role of dynamin-related protein 1, a mediator of mitochondrial fission, in apoptosis. Developmental cell. 2001;1(4):515–25.
39. Green DR, Kroemer G. The pathophysiology of mitochondrial cell death. Science. 2004;305(5684):626–9.
40. Elmore S. Apoptosis: a review of programmed cell death. Toxicologic pathology. 2007;35(4):495–516.
41. Mohammadinejad R, Moosavi MA, Tavakol S, Vardar DÖ, Hosseini A, Rahmati M, et al. Necrotic, apoptotic and autophagic cell fates triggered by nanoparticles. Autophagy. 2019;15(1):4–33.
42. Creagh EM, Conroy H, Martin SJ. Caspase-activation pathways in apoptosis and immunity. Immunological reviews. 2003;193(1):10–21.
43. Gogolák P, Réthi B, Hajas G, Rajnavölgyi É. Targeting dendritic cells for priming cellular immune responses. Journal of Molecular Recognition. 2003;16(5):299–317.
44. Li P, Gregg JL, Wang N, Zhou D, O'Donnell P, Blum JS, et al. Compartmentalization of class II antigen presentation: contribution of cytoplasmic and endosomal processing. Immunological reviews. 2005;207(1):206–17.
45. Tonigold M, Mailänder V. Endocytosis and intracellular processing of nanoparticles in dendritic cells: routes to effective immunonanomedicines. Taylor & Francis; 2016. p. 2625–30.
46. Boraschi D, Costantino L, Italiani P. Interaction of nanoparticles with immunocompetent cells: nanosafety considerations. Nanomedicine. 2012;7(1):121–31.
47. Li L, Yan X, Xia M, Shen B, Cao Y, Wu X, et al. Nanoparticle/nanocarrier formulation as an antigen: the immunogenicity and antigenicity of itself. Molecular Pharmaceutics. 2021;19(1):148–59.
48. Baljon JJ, Wilson JT. Bioinspired vaccines to enhance MHC class-I antigen cross-presentation. Current opinion in immunology. 2022;77:102215.
49. Zhang W, Wang L, Liu Y, Chen X, Liu Q, Jia J, et al. Immune responses to vaccines involving a combined antigen–nanoparticle mixture and nanoparticle-encapsulated antigen formulation. Biomaterials. 2014;35(23):6086–97.
50. Liang J, Yao L, Liu Z, Chen Y, Lin Y, Tian T. Nanoparticles in Subunit Vaccines: Immunological Foundations, Categories, and Applications. Small. 2025;21(1):2407649.
51. Mundekkad D, Cho WC. Nanoparticles in clinical translation for cancer therapy. International journal of molecular sciences. 2022;23(3):1685.

© 2025 by the author(s). Distributed under a Creative Commons CC BY license.

Preprints.org (www.preprints.org) | NOT PEER-REVIEWED | Posted: 12 May 2025 doi:10.20944/preprints202505.0830.v1

52. Lee IH, Kwon HK, An S, Kim D, Kim S, Yu MK, et al. Imageable antigen-presenting gold nanoparticle vaccines for effective cancer immunotherapy in vivo. Angewandte Chemie-International Edition. 2012;51(35):8800.
53. Silva JM, Gaëlle V, G. OV, N. PS, Catarina R, Ana S, et al. Development of Functionalized Nanoparticles for Vaccine Delivery to Dendritic Cells: A Mechanistic Approach. Nanomedicine. 2014;9(17):2639–56.

Disclaimer/Publisher's Note: The statements, opinions and data contained in all publications are solely those of the individual author(s) and contributor(s) and not of MDPI and/or the editor(s). MDPI and/or the editor(s) disclaim responsibility for any injury to people or property resulting from any ideas, methods, instructions or products referred to in the content.

© 2025 by the author(s). Distributed under a Creative Commons CC BY license.